CCFE
CULHAM CENTRE FOR FUSION ENERGY

CCFE-PR(15)12

A. De Backer, G. Adjanor, C. Domain, M.L. Lescoat, S. Jublot-Leclerc,
F. Fortuna, A. Gentils, C. J. Ortiz, A. Souidi, C.S. Becquart

Modeling of Helium Bubble Nucleation and Growth in Austenitic Stainless Steels using an Object Kinetic Monte Carlo Method

Modeling of Helium Bubble Nucleation and Growth in Austenitic Stainless Steels using an Object Kinetic Monte Carlo Method

A. De Backer[1*], G. Adjanor[2], C. Domain[2], M.L. Lescoat[2], S. Jublot-Leclerc[3], F. Fortuna[3], A. Gentils[3], C. J. Ortiz[4], A. Souidi[5], C.S. Becquart[6]

[1]CCFE, Culham Centre for Fusion Energy, Abingdon, Oxon, United Kingdom
[2]EDF R&D, MMC Centre des Renardières, Moret-sur-Loing, France
[3]CSNSM, Paris-Sud, CNRS/IN2P3, Orsay, France
[4]CIEMAT, Laboratorio Nacional de Fusión por Confinamiento Magnético, Madrid, Spain
[5]Université Dr. Tahar Moulay de Saida, Saida, Algeria
[6]UMET, UMR 8207, Université Lille 1, Villeneuve d'Ascq, France

The following article was published in Nuclear Instruments and Methods in Physics Research Section B: Beam Interactions with Materials and Atoms, Vol.352, 1 June 2015, pp.107-114

Modeling of Helium Bubble Nucleation and Growth in Austenitic Stainless Steels Using an Object Kinetic Monte Carlo Method

A. De Backer[1*], G. Adjanor[2], C. Domain[2], M.L. Lescoat[2], S. Jublot-Leclerc[3], F. Fortuna[3], A. Gentils[3], C. J. Ortiz[4], A. Souidi[5], C.S. Becquart[6]

[1] *CCFE, Culham Centre for Fusion Energy, Abingdon, Oxon, United Kingdom*
[2] *EDF R&D, MMC Centre des Renardières, Moret-sur-Loing, France*
[3] *CSNSM, Paris-Sud, CNRS/IN2P3, Orsay, France*
[4] *CIEMAT, Laboratorio Nacional de Fusión por Confinamiento Magnético, Madrid, Spain*
[5] *Université Dr. Tahar Moulay de Saida, Saida, Algeria*
[6] *UMET, UMR 8207, Université Lille 1, Villeneuve d'Ascq, France*

*Corresponding author: andree.debacker@ccfe.ac.uk

Abstract
Implantation of 10 keV helium in 316L steel thin foils was performed in JANNuS-Orsay facility and modelled using a multiscale approach. Density Functional Theory (DFT) atomistic calculations [1] were used to obtain the properties of He and He-vacancy clusters, and the Binary Collision Approximation based code Marlowe was applied to determine the damage and He-ion depth profiles as in [2,3]. The processes involved in the homogeneous He bubble nucleation and growth were defined and implemented in the Object Kinetic Monte Carlo code LAKIMOCA [4]. In particular as the He to dpa ratio was high, self-trapping of He clusters and the trap mutation of He-vacancy clusters had to be taken into account. With this multiscale approach, the formation of bubbles was modelled up to nanometer-scale size, where bubbles can be observed by Transmission Electron Microscopy. Their densities and sizes were studied as functions of fluence (up to 5×10^{19} He/m^2) at two temperatures (473 K and 723 K) and for different sample thicknesses (25 – 250 nm). It appears that the damage is not only due to the collision cascades but is also strongly controlled by the He accumulation in pressurized bubbles. Comparison with experimental data is discussed and sensible agreement is achieved.

Keywords: helium, damage, bubble, self-trapping, trap mutation, austenitic stainless steel, multiscale modeling;

1. Introduction

In the internal components of the present generation nuclear reactors, helium can be produced due to transmutation reactions. In service conditions, helium production is small. However, real conditions vary widely from in service condition to the different experimental reactors and numerical modeling is necessary to predict the long term evolution of steel microstructure. These models need to be validated using dedicated ion irradiation experiments, leading to non activated samples. The CoIrrHeSim project [5] aims to study three conditions using the dual ion beam in-situ TEM facility JANNuS-Orsay: He beam only, He-damage dual beam and damage only beam. This work reports experimental and modeling results of the He-only implantation of 316L steel thin foils. In these extreme conditions, helium accumulates on microstructure defects and precipitates into bubbles. After a short presentation of some experimental results, the multiscale model is described. Finally, simulation results obtained at 473 K and 723 K are presented and analyzed.

2. Experimental results

In-situ 10 keV He ion implantations were performed on 316L austenitic stainless steel thin foils in the JANNuS-Orsay facility at two elevated temperatures, namely 473 K and 723 K, to a fluence of 5×10^{19} m^{-2}. At 473 K, very small bubbles at the limit of detection (< 0.8 nm) are observed as revealed by the opposite white/black contrast in

under and over focus conditions shown on Fig 1a (some of the visible bubbles have been circled in red). It is very likely that a high concentration of smaller bubbles have formed in the sample. These small bubbles are either not visible due to detection limits or not distinguishable from an amorphous oxide layer that has formed on top of the specimen and which gives a similar black/white contrast. For these reasons, it was not possible to determine their concentration.

At 723 K, a large concentration of bubbles is clearly visible (Fig. 1b) and their size ranges from 1.0 to 2.7 nm. Their concentration was estimated to a value between 4.8 and 5.8 × 10^{23} bubbles/m^3 in a 60 nm thick region. The same range of concentration was obtained in a thicker region (90 nm). At lower thicknesses of the thin foil, lower concentrations were obtained showing a "free surface effect" which was obvious in regions thinner than 40 nm where no bubble was observed. No extended defects such as dislocation loops were observed. From our experimental investigations as well as previous experimental works on the subject [6], we concluded that the higher the implantation temperature, the lower the nucleation but the larger the bubbles.

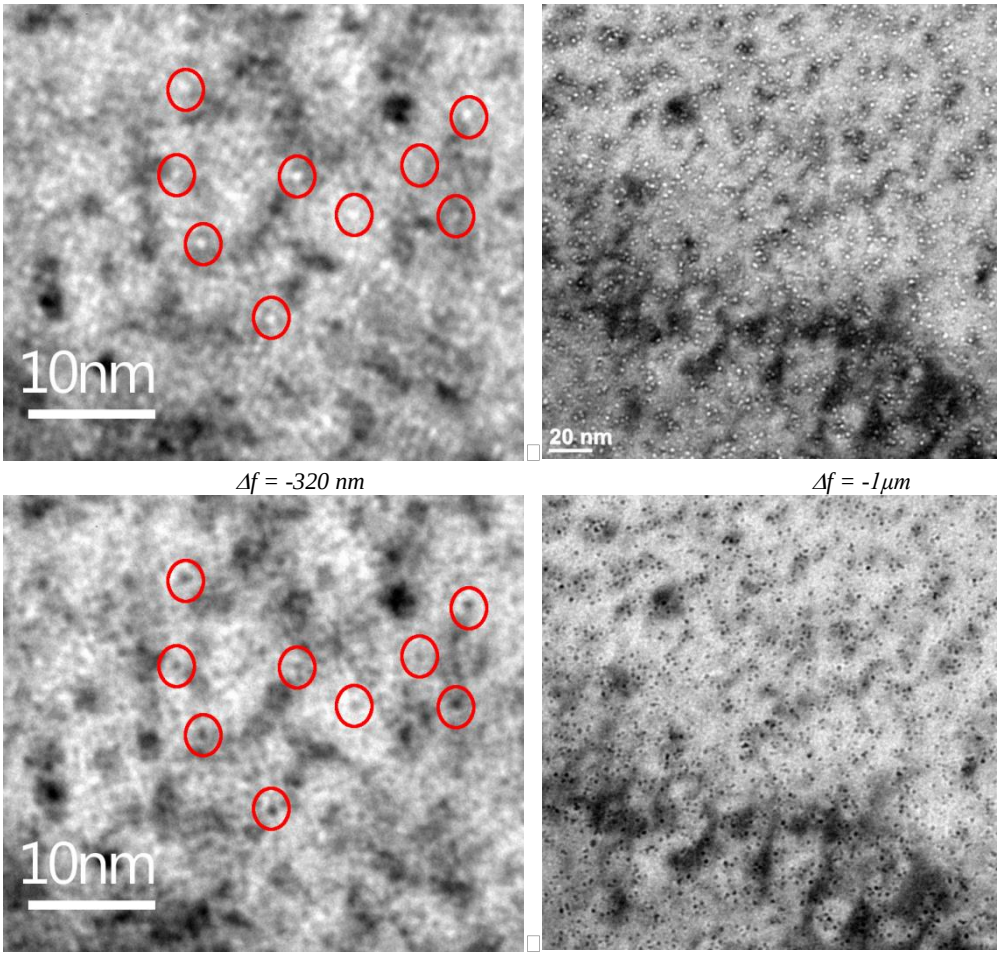

Δf = -320 nm *Δf = -1μm*

Δf = +320 nm *Δf = +1μm*

(a) *(b)*

Fig. 1. TEM bright-field images of He bubbles in 10 keV He ion implanted 316L at 473 K; (b) at 723 K. Δf is the value of the defocus used. Bubbles appear white at a negative Δf, and black at a positive Δf.

3. He implantation and He-point defects interaction modeling

For this work, the multiscale approach that we adopted mainly consists in 1\ the evaluation of the damage using the MARLOWE code based on the Binary Collision Approximation (BCA), 2\ the description of the processes

(diffusion, recombination and clustering of defects and helium atoms) implemented in the OKMC model and 3\ the development of a parameterization based on Density Functional Theory (DFT) calculations from [1] for the thermally-activated processes taken into account in the OKMC.

3.1 Evaluation of the damage: the displacement cascades

MARLOWE is based on the BCA and makes possible the elimination of unstable created Frenkel (FP) pairs using a critical distance called recombination radius. This method mimics remarkably well the different processes that occur during the thermal spike and replacement sequences and has been applied in BCC iron and W [2]. For this project, 10 keV He cascades in a FeNiCr FCC lattice were calculated. The amount of FP as a function of their separation distance is shown Fig 2a. It decreases rapidly from 15 to 1 for a recombination radius of 5 lattice units. To determine the recombination radius, the same method used in Fe and W was applied by comparing the damage predicted by MARLOWE to Primary Knock-On Atom (PKA) cascades calculated using Molecular Dynamics (MD) [7]. The MD cascades were obtained with a FeNiCr potential derived in [8] and hardened in the framework of the PERFORM-60 project [9]. A recombination radius equal to $4a_0$ lattice unit was chosen which gives on average 1.2 Frenkel Pairs (FP) per 10 keV He.

30,000 Marlowe cascades were then calculated at 473 K and 723 K and post processed using this recombination radius. The comparison with SRIM [10] (using a displacement energy of 40 eV and the "monolayer" option) is illustrated Fig 2b. Both Marlowe and SRIM predict similar implantation (~ 50 nm) and damage (~ 20 nm) peaks. MARLOWE takes into account the crystal structure and predicts some channelling which causes a deeper penetration of the He atoms. The main difference is the amount of FP per He atom: SRIM predicts 38 FP per He atom while Marlowe predicts 1.2 FP on average. MARLOWE also gives details on the cascade: 1/3 of them contain only one He atom, 1/3 contains one He and one FP and the last third contains one He and 2-4 FP.

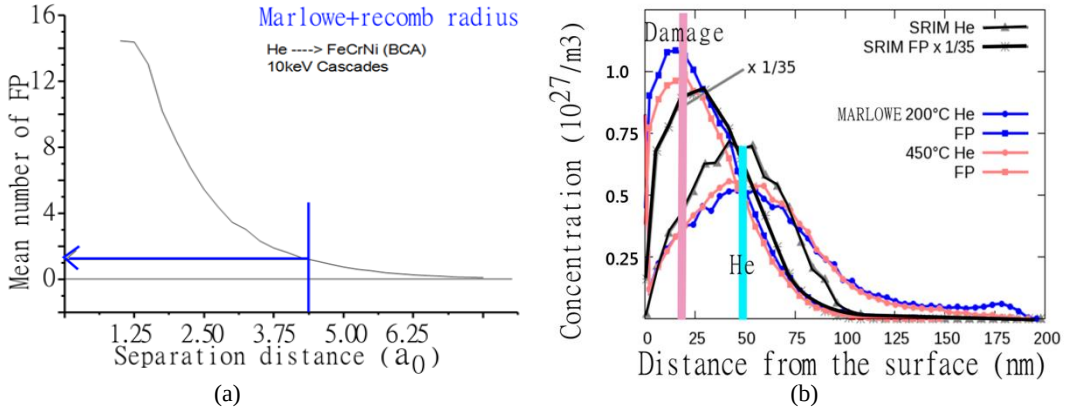

(a) (b)

Fig. 2. (a) mean number of stable FP per cascade as a function of the recombination radius adjusted to reproduce the thermal spike and replacement sequences; (b) damage and ion peaks predicted by SRIM (displacement energy of 40 eV) and Marlowe (recombination radius of 4 lattice parameter, a_0) for the maximum fluence of 5×10^{19} He/m^2

3.2 OKMC simulations

Our OKMC simulations have been done with LAKIMOCA [4]. One considers a box where defects and He-ions are introduced to mimic the He implantation. As the time moves forward, events are realized according to the residence time algorithm [11]. Possible events are jumps of objects, emission of entities from clusters or external events, which in this case are the introduction of a new cascade (with a probability given by the He flux used in the experiment). After each random event, the vicinity of defects that have moved is inspected. If another defect is found within a distance smaller that the capture radius, then it is assumed that a reaction instantaneously takes place.

In previous works, we modelled conditions where He was implanted together with a lot of defects, (i.e. many vacancies and SIAs), the main nucleation and growth mechanisms of bubbles (or rather voids containing He atoms) was the clustering of vacancies and in some conditions He atoms enhanced the nucleation [12]. In this work, the

damage produced by the slowing down of He atoms is very low and is expected to decrease because of the recombination that takes place when SIAs and vacancies diffuse as modelled with the OKMC. To treat bubble nucleation and growth, we had to implement new events: the self-trapping and trap mutation processes investigated recently using DFT and MD methods in W [13,14]. The self-trapping process occurs if one large nHe cluster, which is mobile and diffuses in the bulk, turns into a nHe.V.SIA complex by creating a vacancy, sitting inside and pushing a metal atom nearby. The nHe.V.SIA cluster is then immobile. A second thermally activated process can take place if the pushed atom goes far away from the nHe.mV cluster and becomes a free SIA described by the reaction nHe.V.SIA → nHe.V + SIA. The trap mutation process is similar to the self-trapping process but happens to a nHe.mV (or nHe.mV.pSIA) cluster that is pressurised by enough He to turn into a nHe.(m+1)V.(p+1)SIA. By this process, bubbles can grow.

A drawing picture of the reactions involving the new complex nHe.V.pSIA in the OKMC is given on Fig 3. One can see the emission of one He atom and one vacancy (a', b'), the trap mutation process (c') and dissociation of the nHe.mV and pSIA part of the complex. They are considered as thermally activated while the reactions with diffusing species are controlled by a capture radius. The nHe.mV part can accumulate He (a) and vacancy (b) and shrinks by recombining with SIA (c). The SIA cluster part can grow or shrink by reacting with SIAs (g) and vacancy (f), respectively. For this work, the dissociation of the nHe.mV.pSIA in nHe.mV and pSIA was not considered (d'). Furthermore, the pSIA part of the nHe.mV.pSIA complex is not expected to become very large thus the trapping of He or emission of a SIA were neglected (e, g').

These simplifications were made, as our aim is to put in evidence the role of the trap mutation process in limiting the He to vacancy ratio in the nHe.mV.pSIA complexes (related to the He density, thus the He pressure) and controlled by a thermally activated process whose energy decreases when the He atoms accumulate.

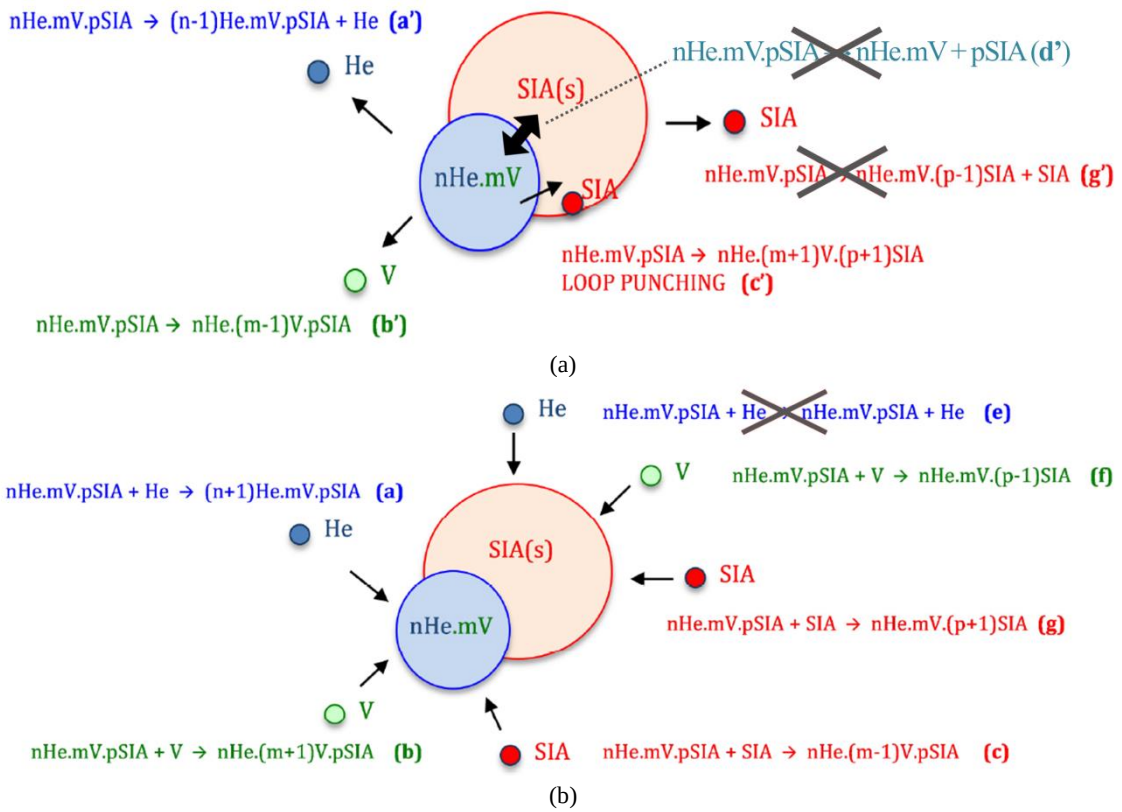

Fig. 3. (a) thermally activated reactions involving the newly implemented nHe.mV.pSIA complex; (b) reverse processes limited by a distance criteria between the new nHe.mV.pSIA complex and the mono objects. Reactions (a, b and c) were already implemented and reactions (c', f and g) have been added but (e, d' and g') are neglected for the moment

3.3 Parameterization

In our model, He atoms and small He clusters are mobile with a migration energy equal to 0.41 eV as in [15] that refers to [16] (and resp. 0.69 and 1.0 eV for the 2He and 3He clusters). The prefactors for the He and He cluster diffusion have been chosen equal to 6×10^{12} s^{-1}. The prefactors for the vacancy and SIA diffusion have been chosen in order to correspond to diffusion coefficients, and the prefactors for the defect and He emission have been chosen as a function of the capture radius to follow the continuous law of diffusion in steady state as described in [17]. The capture radius increases with the object size and is 0.3 nm for the He atom. The parameterization of He clusters is based on DFT calculations from [1]. The first process is the He release from a nHe cluster: He atom (nHe → (n-1)He + He). Using the dissociation model, the activation energy is:

$$E_a(\text{He; nHe}) = E_f((n-1)\text{He}) + E_f(\text{He}) - E_f(\text{nHe}) + E_m(\text{He}) = E_b(\text{He; nHe}) + E_m(\text{He})$$

where E_b, E_m, E_f designate binding, migration and formation energies respectively.

The second process is self-trapping: nHe → nHe.V.SIA. The calculation of the activation energies requires further investigations of He properties that are not existing for this material (to our knowledge) but that we investigated in W[13]. For this work, although it is debatable, in lack of atomistic data, we used a simple dissociation model and we confused the self-trapping process and the SIA emission. These two processes are different and are referred to the following reactions: nHe → nHe.V.SIA and nHe → nHe.V + SIA. The activation energies are calculated as

$$E_a(\text{ST; nHe}) = E_f(\text{SIA}) + E_f(\text{nHe.V}) - E_f(\text{nHe}) + E_m(\text{SIA})$$
$$= E_f(\text{SIA}) + E_f(\text{V}) - E_B(\text{nHe.V}) + E_B(\text{nHe}) + E_m(\text{SIA})$$

where the binding energies refer now to the "total" dissociation of the cluster: $E_B(\text{nHe.V}) = n\,E_f(\text{He}) + m\,E_f(\text{V}) - E_f(\text{nHe.V})$. We are aware that this terminology can be sometimes confusing but it corresponds to what is used in many papers.

The obtained values are reproduced in Fig 4a as a function of the number of He atoms in the He cluster. It can be observed that the larger the cluster the lower the probability of He release and the higher the probability of self-trapping. According to this parameterization, no He cluster containing more than 4 - 5 helium atoms can persist a long time in the simulation: using an Arrhenius formula at room temperature, the probability of self-trapping of one 4He is 5×10^{12} s^{-1}.

The nHe.mV (and nHe.mV.pSIA) clusters are all immobile. They can undergo three thermally activated processes: emission of one vacancy, emission of one He atom and trap mutation. The activation energies were calculated using the dissociation model with migration energies respectively equal to 1.0 eV, 0.5 eV and 0.41 eV for the vacancy, SIA and He atom, respectively. Similarly to self-trapping, the trap mutation (TM) activation energies, with debatable hypotheses, are calculated as

$$E_a(\text{TM; nHe.mV}) = E_a(\text{TM; nHe.mV.pSIA}) = E_f(\text{SIA}) + E_f(\text{nHe.(m+1)V}) - E_f(\text{nHe.mV}) + E_m(\text{SIA})$$
$$= E_f(\text{SIA}) + E_f(\text{V}) - E_b(\text{V;nHe.(m+1)V}) + E_m(\text{SIA})$$

For the large nHe.mV clusters whom dissociation energies have not been calculated by DFT, for example for clusters containing more than 4 vacancies and more than 6 helium atoms, extrapolation formulas were fitted on the dissociation energies versus He to vacancy ratio. The results are illustrated in Fig 4b. The three process probabilities respectively decrease for the vacancy emission and increase for the He emission and the trap mutation, with the He to vacancy ratio. This is explainable considering that the He to vacancy ratio is related to the He pressure: when the He pressure in the bubble increases, the vacancy emission is inhibited, the He release is enhanced and above a certain level, the pressure release by increasing the bubble volume becomes energetically favourable.

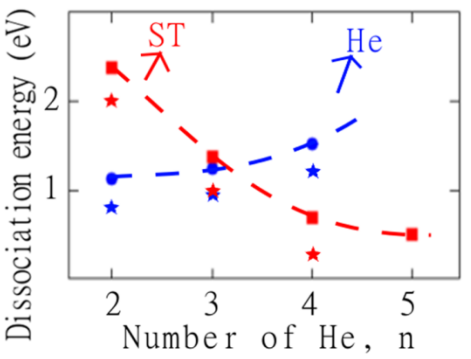

(a)

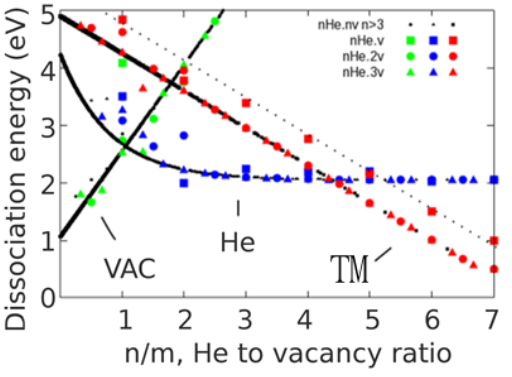

(b)

Fig. 4. (a) activation energies for the emission of one He atom and self-trapping of the nHe clusters; (b) activation energies for the emission of one vacancy or one He atom and trap mutation of the mixed nHe.mV and nHe.mV.pSIA clusters

The monovacancy and monoSIA are mobile and their migration energies are respectively 1.0 eV and 0.5 eV. They were found [18] to be the most adequate to reproduce the experimental results of [19,20]. Defect clusters are immobile and the activation energies for the emission of single entities are calculated using the dissociation model and capillarity laws as in [21]

$$E_a(\text{Def; nDef}) = E_f((n\text{-}1)\text{Def}) + E_f(\text{Def}) - E_f(n\text{Def}) + E_m(\text{Def})$$
$$= E_f(\text{Def}) + (E_b(\text{Def;2Def}) - E_f(\text{Def}))/(2^{2/3}-1) \times (n^{2/3} - (n-1)^{2/3}) + E_m(\text{Def})$$

where the binding and formation energies are the one calculated in [1] $E_f(\text{SIA}) = 3.2$ eV, $E_f(\text{V}) = 1.81$; $E_b(\text{SIA;2SIA}) = 0.9$ eV and $E_b(\text{V;2V}) = 0.18$ eV.

SIA clusters are not expected to grow up to form dislocation loops and vacancy clusters contain many He atoms in the investigated conditions as the amount of damage in the cascades is low and no extended defects are visible in the experimental observations. If this was not the case, attention should be paid to this aspect of the parameterization as in [22].

4. Modeling results

He implantations were first performed at 473 K up to a fluence of 5×10^{19} He/m^2. Different box sizes and box thicknesses were tested. He retained fraction, remaining vacancy and SIA fractions and the permanent damage due to the self-trapping and trap mutation processes are illustrated in Fig 5 as a function of fluence. It can be observed that when the fluence increases the retained He fraction increases, which is expected as bubbles form and are efficient traps for additional He atoms; thus their probability to reach the surface decreases. The opposite tendencies are observed on the SIA and vacancy remaining fractions as they have an increasing probability to recombine. The SIA fraction is lower because they are much more mobile than vacancies and thus are eliminated at the surface more efficiently. What is more interesting is the "permanent damage" due to self-trapping and trap mutation processes happening to the nHe and nHe.mV clusters. Because of those processes, the averaged He to vacancy ratio was found around 5. It is related to the He density in the bubble or the He pressure and determined by our parameterization. SIA recombination with the vacancy part of the cluster is not energetically favourable and the accumulation of He causes bubbles to grow.

The thickness sample impacts the bubble concentration as the back surface progressively erodes it. On Fig 5b, one can see that roughly 4 times less bubbles formed in a 25 nm thick sample compared to a 100 nm thick sample. Around 1.5×10^{24} bubble/m^3 of 1 nm size on average have been obtained. As explained in the section 2, in the experiment, a lot of bubbles were visible but it was not possible to estimate their density as their sizes were at the limit of detection (< 0.8 nm). With our model we found a large number of bubbles but it seems that we overestimate the bubble size. One reason can be the underestimation of the He + V $\rightarrow$ He.V nucleation process, thus the underestimation of the density of bubbles and thus the overestimation of their mean size. The underestimation of the He + V $\rightarrow$ He.V nucleation process can be due to the high fraction of eliminated FP in He cascades during the post processing described in section 3.1. However an increase of the number of FP in the cascades also implies an increase of the number of SIAs and there are no simple speculations on the effect this would have on the results. Additional simulations are in progress to clarify this issue.

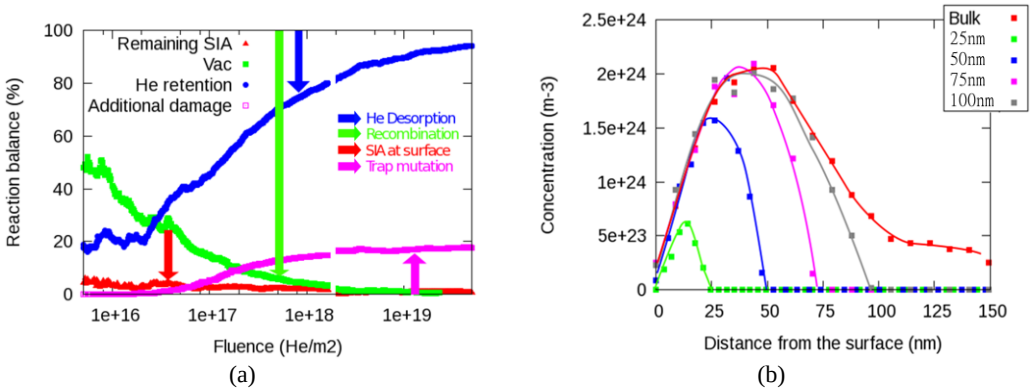

(a) (b)

Fig. 5. (a) retained He and remaining vacancies and SIA fractions respectively divided by the number of introduced He, vacancies and SIAs, as a function of He fluence as well as the damage due to the bubble formation calculated as the number of vacancies created by self trapping and trap mutation processes divided by the number of vacancies created by introduction of cascades. By complementarity the arrows directly indicate the He desorption, vacancy-SIA recombination, SIA elimination at the surface and the trap mutation fraction; (b) final bubbles concentration as a function of distance from the surface for different box thicknesses (25, 50, 75, 100, 250 nm). These simulations have been done at 473 K and the final fluence is 5×10^{19} *He/m*^{2}.

Simulations at 723 K are illustrated on Fig 6. The effect of the sample thickness is qualitatively different from what was observed at 473 K: now a thickness threshold exists as no bubble is formed in 50 nm thick and thinner samples. At this high temperature, the simulations are very CPU consuming because the nHe.mV clusters dissociate frequently. For a 75 nm thick sample, the prediction of the bubble concentration is around 10^{23} bubble/m^3 which is only 5 times less than the experimental results and their mean size is around 1 nm which is slightly underestimated.

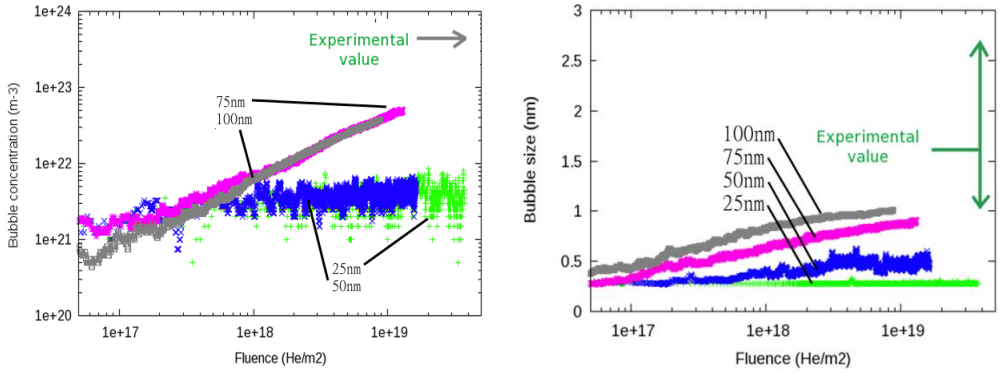

(a) (b)

Fig. 6. (a) bubble concentration as a function of He fluence for different box thicknesses at 723 K; (b) and mean bubble size.

We analysed the origin of the small size of the bubbles at 723 K in our model. They appear to be unstable because the He emission probability becomes important at high temperature and this whatever their size. The cause is the simple extrapolation formula that depends only on the He to vacancy ratio (see Fig 4) and are at odds with the properties of bubbles that says that the larger the bubble the more stable they are. In this project, it became obvious that this property has to be taken into account for the modeling of high temperature implantations. One point of view is that when the bubble grows the surface energy becomes less and less penalising as it is also observed for SIA and vacancy clusters. Another reason is that when the bubble grow, the penalizing He-metal interaction becomes less important as described in [23]. Investigations of these aspects by DFT and MD in W are reported in [13,14]. For this work, we simply added a term of 0.05 eV per vacancy to the binding energy of nHe.mv clusters, using estimation from MD simulations in pure bcc Fe done for the adjustment of the "variable gap" model and reported in [24]. The schematic drawing of the effect on the activation energies is illustrated Fig 7 with arrows, blue for the emission of He and pink for the trap mutation. In the same figure, two lines are traced respectively for 473 K and 723 K. They estimate the threshold between activated and unactivated processes at those temperatures: processes corresponding to activation energy below the line are activated and the corresponding clusters cannot persist in the simulation box. It can be deduced that at 723 K, when a He.V nucleus accumulates He atoms, it goes through unstable states and the release of trapped He is highly probable until trap mutation takes place which decreases the He to vacancy ratio (and eases more He accumulation). With the additional term depending on the number of vacancies, related to the bubble size, trap mutation brings the nHe.mV to a more stable curve (dotted lines). With this term, the more the bubbles grow, the more stable they are and the easier the He accumulation. The bubble sizes predicted by the OKMC with the new parameterization are illustrated Fig 7b and overpass the experimental estimations. This proves how important is taking into account that the larger the bubble the more stable they are for the modeling of bubble nucleation and growth at 723 K.

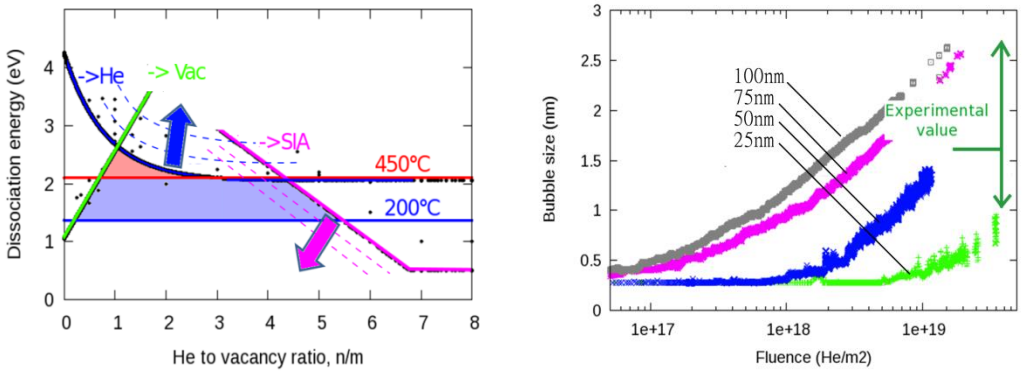

(a) (b)

Fig. 7. (a) schematic drawing of dissociation energies with the additional term depending on the cluster size, i.e. the number of vacancies; (b) mean bubble size as a function of He fluence at 723 K for different thicknesses and with the new parameterization.

5. Discussion

In this model the migration energy of the interstitial He has been chosen higher than common values obtained by DFT in alpha iron [25] or in tungsten [26] which is also a bcc material. The energy barrier for the He diffusion in fcc iron has been recently investigated by DFT in [1] and was found to be not only higher than in bcc Fe, but also to be highly dependent on the magnetic environment (from 0.16 eV to 0.35 eV as given in table VII of [1]). In the OKMC simulations, when the lowest value of [1] i.e. 0.16 eV was used, no bubble was formed at 723 K. We then tested a higher value of 0.41 eV, which has been used in [15] in a Cluster Dynamics model and gave good agreement with experimental data. This higher migration energy did not affect the simulation at 473 K but it allowed the nucleation of He bubbles at 723 K as observed in the experiment. The reason is that this higher migration energy shifts up the He dissociation energy and stabilizes thus the small He clusters and He-vacancy clusters. With large scale models it is not uncommon that one has to increase the migration energy of diffusing species obtained in pure and perfect materials using DFT calculations, to be able to reproduce real experiments. This is usually interpreted as the effect of impurities or other elements of real materials microstructure.

Recently, another mechanism has been revealed that is not introduced in our model and can also explain the inhibition of the growth of the small He bubbles at 473 K. Using Molecular Dynamics and Kinetic Monte Carlo methods, Gai et al. [27] studied the energy barriers of He in bcc iron to join the pressurized bubbles and found that they become very large for pressurized bubbles. Consequently, the bubble growth by helium accumulation becomes very unlikely at low temperature and small bubbles can only grow by the addition of vacancies from a cascade. The implementation of this new mechanism is an interesting perspective for this work and would clarify the importance of the different processes in different conditions.

To prevent any ambiguity in our arguments, the modeling of the He implantation at 473 K has been done with the parameterization that takes into account the size effect on the stability of the He-vacancy clusters. At 473 K, the He-vacancy cluster lifetimes are longer than the other characteristic times in the simulation. A slight increase of their dissociation energies does not change the balance between the different processes. However the new parameterization also shifts down the characteristic curve of the trap mutation when the He-vacancy cluster size increases (as illustrated on Fig. 7). In comparison with the simulations done with the parameterisation that does not take into account the effect of the cluster size on the binding energies, the new simulations revealed no noticeably difference on the bubble concentration and mean size but a slight broadening of the He-vacancy cluster distributions. However the study of the bubble size distribution is out of the scope of this work and would probably require the introduction of the mechanism described in [27], i.e. the inhibition of the bubble growth by the increase of the barrier for the He to join the bubble.

Our investigations suggest a sensitivity of our multiscale approach to the He to vacancy ratio in the cascades predicted by MARLOWE and its discrepancy with established Binary Collision Approximation model for amorphous materials (such as SRIM [10]). Even though this issue is not the subject of this paper, it requires to be discussed. The

slowing down of ion in matter has been studied for many years using the BCA and the limitations of the models are well known [28]. Molecular Dynamic simulations are also useful predictive tools. However MD and BCA approaches are based on empirical potentials to model the forces between the ions as a function of the mutual distance. The MARLOWE code is one BCA approximation of Molecular Dynamics. It calculates the trajectory of the ion and all the recoils that it produces in a crystal lattice but using the scattering integral given by the BCA instead of the real time integration of the forces given by the empirical potentials. In BCA and full MD approaches, the empirical potentials are usually the same in the short range part that is relevant for the ballistic stage of the cascade. The usefulness of the full MD simulation relies on the development of accurate and more complex potentials on their mid and long range parts that reproduce correctly the collective interactions of the atoms. To our knowledge there were no such accurate potentials for the He interaction in fcc iron based alloys during the course of this work. The MARLOWE model has been studied and improved in bcc iron to better reproduce the collective processes observed in full MD [29-31]. It has also be done in W for the He implantation [2,4] where it was proven to be more accurate than SRIM, as SRIM does not take into account the crystalline structure of materials, and thus neglects completely channeling effects for instance. Another advantage of MARLOWE is that it accounts for recombination of interstitials and vacancies during thermal spike, using a capture radius adjusted on MD results. The number of Frenkel pairs calculated by MARLOWE is thus, in principle, in good agreement with what MD would predict. One aspect of this project was to use new results using MARLOWE and adjusted parameters on full MD (but without helium) using the most recent potentials for the FeNiCr system. More details are out the scope of this paper but more information will be available in this journal [7]. In this paper we report our study of the sensitivity of the multiscale model as a whole and we observed that the He to vacancy ratio is a crucial parameter of the model. Our results suggest that the reason why the accuracy of the He to vacancy ratio in the cascades is important is the competition between the nucleation of bubbles by nHe cluster formation and by He accumulation in the vacancies that did not recombine with the SIAs. In that sense this work illustrates the sensitivity of the model as a whole and justifies the current work on the adjustment of MARLOWE parameters and the development of FeNiCr potentials for cascade calculations as reported in [8,9]. Furthermore is it not simple to speculate on the effect of the increase of the number of SIAs in the cascade and works are in progress to clarify this issue.

This work describes problems that one faces when one develop a multiscale approach and it opens perspectives. Beside the problems of the self trapping and trap mutation (which should be further investigated in this materials as it has been done in W [13,14]) and the complex barrier for the He to join the bubble, as studied in [27], other recent and interesting works illustrate the complexity of this material due to the variability of the local environment [32] which leads to the multiplicity of the formation energies. Indeed, our approach cannot deal with the complexity of the atomistic local effects that require to be investigated by other methods. Other example of OKMC methods handling complex systems exist [33,34]. Similarly our OKMC is not limited in the number and the complexity of the processes implemented and enables the study of their relative impact on the kinetic evolution of long term simulations. We reported in this paper our first results in that regard.

6. Conclusion

We reported in-situ TEM observations of small He bubbles, close to the limit of detection, in He implanted 316L austenitic stainless steel at 473 K and 723 K. From experimental investigations, we concluded that the higher the implantation temperature, the lower the nucleation but the larger the bubbles. We developed a multiscale model of the He bubble nucleation and growth under low damage to He ratio conditions. The two He implantations at low and high temperatures have been simulated and compared with the experimental results. This model incorporates the competition between different nucleation processes: He accumulation in vacancy clusters and He cluster self-trapping. Our results suggest the sensitivity of our model to the He to vacancy ratio in the damage produced during the slowing down of the He ions. For this work, MARLOWE has been adjusted on MD cascades and predicted a lower He to vacancy ratio that BCA model for amorphous material as SRIM but further works are necessary to determine the impact on the multiscale model results. However the results proved the great sensitivity of the model at high temperature to the dissociation energy of the small He bubbles. This sensitivity of the model has been related to a "physical" mechanism which is that the small He-vacancy clusters become unstable at high temperature but that their stability increases with their size. The nucleation process becomes less probable and depends on the critic size of the nuclei. In our model this critic size is handled by the increase of the dissociation energies with the He-vacancy cluster size but quantification of this feature needs further investigations using atomistic methods.

Acknowledgments

This work has received a financial support from the French National Research Agency through the project CoIrrHeSim ANR-11-BS09-006. Work performed at UMET and EDF is part of the research program of the EDF-CNRS joint laboratory EM2VM (Study and Modeling of the Microstructure for Ageing of Materials). Work at CCFE was part-funded by the RCUK Energy Programme (Grant Number EP/I501045) and by the European Unions Horizon 2020 research and innovation programme under grant agreement number 633053. To obtain further information on the data and models underlying this paper please contact PublicationsManager@ccfe.ac.uk. The views and opinions expressed herein do not necessarily reflect those of the European Commission. This work was also part-funded by the United Kingdom Engineering and Physical Sciences Research Council via a programme grant EP/G050031. This work contributes to the Joint Programme on Nuclear Materials (JPNM) of the European Energy Research Alliance (EERA). The authors thank particularly Dr. Thomas Jourdan and Dr Sergei Dudarev for fruitful discussions.

References

[1] D.J. Hepburn, D. Ferguson, S. Gardner, G.J. Ackland, *Phys. Rev. B* **88** (2013) 024115.
[2] M. Hou, C. Ortiz, C.S. Becquart, C. Domain, U. Sarkar, A. De Backer, *Jour. Nucl. Mater.* **403** (2010) 89.
[3] C.J. Ortiz, A. Souidi, C.S. Becquart, C. Domain and M. Hou, *Radiation Effects & Defects in Solids*, 2014
[4] C.S. Becquart, C. Domain, *Jour. Nucl. Mater.* **385** (2009) 223.
[5] Co-Influence of Irradiation and Helium gas on swelling of pressurized-water nuclear reactors materials components: experimental and numerical simulations, http://csnweb01.in2p3.fr/coirrhesim/
[6] H. Trinkaus, B.N. Singh, *Jour. Nucl. Mater.* **323** (2003) 229.
[7] A. Souidi, M. Hou, C.S. Becquart, C. Domain, A. De Backer, *COSIRES2014 proceeding, Nuclear Instruments and Methods in Physics Research* B submitted
[8] G. Bonny, D. Terentyev, R. C. Pasianot, S. Ponce and A. Bakaev, *Modelling Simul. Mater. Sci. Eng.* **19** (2011) 085008
[9] Z. Al Touq, PhD thesis Loughborough University 2014
[10] www.srim.org
[11] A. B. Bortz and M. H. Kalos and J. L. Lebowitz, *Journal of Computational Physics* **17** (1975) 10
[12] A. De Backer, P.E. Lhuillier, C.S. Becquart, M.F. Barthe, *Jour. Nucl. Mater.* **429** (2012) 78
[13] J. Boisse, C. Domain, C.S. Becquart, *Jour. Nucl. Mater.* **455** (2014) 10
[14] J. Boisse, A. De Backer, C. Domain, C.S. Becquart, *published soon in Materials Research Society* **29** (2014)
[15] M. Zouari, L. Fournier, A. Barbu, and Y. Bréchet, 15th International Conference on Environmental Degradation of Materials in Nuclear Power Systems-Water Reactors (eds J. T. Busby, G. Ilevbare and P. L. Andresen), John Wiley & Sons, Inc., Hoboken, New Jersey, Canada. (2012) doi: 10.1002/9781118456835.ch143
[16] K. Morishita, R. Sugano, B.D. Wirth, *Jour. Nucl. Mater.* **323** (2003) 243
[17] T. Jourdan, G. Bencteux, G. Adjanor, *Jour. Nucl. Mater.* **444** (2014) 298
[18] A. De Backer, G.A Adjanor, T. Jourdan, unpublished work
[19] B.D. Sharma, K. Sonnenberg, G. Antesberger and W. Kesternich, *Phil. Mag.* **37** (1978) 777
[20] Y. Satoh, S. Abe, H. Matsui, I. Yamagata, *Jour. Nucl. Mater.* **367** (2007) 972
[21] C.S. Becquart, C. Domain, U. Sarkar, A. De Backer, M. Hou, *Jour. Nucl. Mater.* **403** (2010) 75
[22] C. Pokor, Y. Brechet, P. Dubuisson, J.-P. Massoud, A. Barbu, *Jour. Nucl. Mater.* **326** (2004) 19
[23] H. Trinkaus, Radiation Effects **78** (1983) 189
[24] T. Jourdan, J.-P. Crocombette, *Jour. Nucl. Mater.* **418** (2011) 98
[25] C. C. Fu and F. Willaime, *Phys. Rev.* B **72** (2005) 064117
[26] C. Becquart and C. Domain, *Phys. Rev.* B **97** (2006) 196402
[27] X. Gai, R. Smith. S. Kenny, *Jour. Nucl. Mater* 2014 submitted
[28] W. Eckstein, "*Computer Simulation of Ion-Solid Interactions, Springer Series in Material Science,"* Vol. 10, Springer Berlin, Heidelberg 1991
[29] M. Hou, *Nuclear Instruments and Methods in Physics Research* B **187** (2002) 20
[30] M. Hou, A. Souidi, C.S. Becquart, *Nuclear Instruments and Methods in Physics Research B* **196** (2002) 31
[31] C.S. Becquart, A. Souidi, M. Hou, *Phys. Rev.* B **66** (2002) 134104
[32] J.S. Wróbel, D. Nguyen-Manh, M.Yu. Lavrentiev, M. Muzyk, and S.L. Dudarev, Phys. Rev. B submitted
[33] A. Gokhman, M. Caturla, F. Bergner, *Radiation Effects and Defects in Solids: Incorporating Plasma Science and Plasma Technology*, **169** Vol. 3 (2014) 185
[34] D. R. Mason, X. Yi, M. A. Kirk and S. L. Dudarev, *Jour. Phys. Condens. Mater.* **26** (2014) 375701